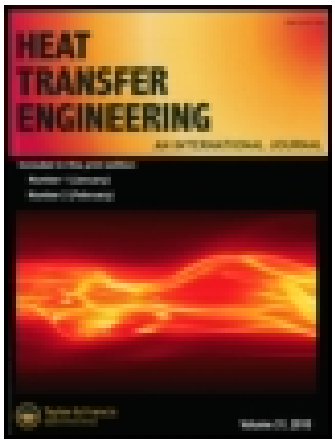

Heat Transfer Engineering
Publication details, including instructions for authors and subscription information:
http://www.tandfonline.com/loi/uhte20

# Study of Thermal Conductivity and Geometry Wall Contact Resistance Effect of Granular Active Carbon for Refrigeration and Heat Pumping Systems

Angeles M. Rivero Pacho[a], Robert E. Critoph[a] & Steven J. Metcalf[a]
[a] School of Engineering, University of Warwick
Accepted author version posted online: 07 Jul 2015.

# Study of Thermal Conductivity and Geometry Wall Contact Resistance Effect of Granular Active Carbon for Refrigeration and Heat Pumping Systems

**Angeles M. Rivero Pacho, Robert E. Critoph, Steven J. Metcalf**

School of Engineering, University of Warwick

Address correspondence to Dr. Angeles M. Rivero Pacho, School of Engineering, University of Warwick, Gibbet Hill Road, Coventry, CV4 7AL, UK. E-mail: A.Rivero-Pacho@warwick.ac.uk



***ABSTRACT***

*The commercial success of sorption refrigeration and heat pump systems depend on a good heat and mass transfer in the adsorbent bed which allows higher coefficients of performance and greater specific heating or cooling power that reduce capital costs. In this study the thermal conductivity and thermal contact resistance of vibrated and compressed granular active carbon and binary mixtures of active carbon are investigated using two types of conductivity measurements: a steady state measurement between flat plates and a transient hot tube measurement. With these results is possible to draw conclusions on how the wall geometry, particle size distribution and bulk density affect the overall thermal performance. Results show that using binary mixtures of grains and powder give superior results to either grains or powder alone. The conductivity of the binary mixtures increases roughly linearly with bulk density and the 2/3 grain mixture achieves the highest densities. The method used to achieve compaction (vibration or compression) did not seem to affect the result. Thermal contact resistances reduce with increasing density but do vary with the mixture ratio, also appearing to be best with a 2/3 grain - 1/3 powder mixture.*

 

## *INTRODUCTION*

The main problem associated with solid adsorbents used in adsorption refrigeration or heat pump systems is their low thermal conductivity. During a refrigeration cycle, the adsorbent has to be heated (desorbing refrigerant) and cooled (adsorbing refrigerant) in order to complete a thermodynamic cycle. The aim of the sorption system development is to achieve a low capital cost by reducing the sorption generator size and reducing cycle time. In order to achieve this, high rates of heat and mass transfer in and out of the adsorbent are critical. To improve the heat transfer and as a consequence, the sorption process of the adsorbent, it is important to increase its thermal conductivity and reduce its thermal contact resistance with the walls of the heat exchanger without increasing the thermal capacity of the generator or reducing its mass transfer.

The solid adsorbent studied in this paper is activated carbon and it is mainly utilised with adsorbates such as ammonia or methanol [1]. Experimental tests show that beds of granular active carbon with ammonia have a typical density of 500 kg/m$^3$ and thermal conductivity value of 0.165 W/(mK) (with minor changes due to concentration). This value contrasts with the individual carbon grains' thermal conductivity, at least five times higher, 0.85 W/(mK), depending on the adsorbate concentration [2].

Active carbon is the chosen adsorption material studied here since it has the advantages of having a stable adsorption performance, a high mass transfer performance, is totally non-volatile (unlike most liquid absorbents) and does not corrode metals as some chemical adsorbents such as chlorides do.

Many approaches have been developed to improve the global heat transfer within the solid adsorbent. Among them is the use of binders or coating materials [3], impact compression [4] and the use of graphite, metallic foams (copper, nickel) [5] or fins [3].

The problem with all these techniques is that the carbon requires high levels of compression and in some sorption generators geometries it is not physically possible to compress it.

In this paper the thermal conductivity and wall thermal resistance of different vibrated binary mixtures of active carbon grains and powder have been studied and tested using both steady and transient techniques with different wall geometries. The aim is to confirm if both techniques obtain the same results and identify for different binary mixtures and different densities how the wall contact resistance affects the effective thermal conductivity of the samples. Some samples have also been mechanically compressed to study if the compression is critical to improve the thermal properties of the adsorbent.



## *EXPERIMENTAL SET UP DESCRIPTION*

In order to measure the thermal conductivity and thermal resistance of the carbon two different methods were used: a steady state method that measures thermal conductivity between flat plates and a transient method that uses a hot tube technique.

### Steady State Flat Plate Measurement

The effective thermal conductivity of the carbon samples were measured following the ASTM E1530 – 11 Standard Test Method the Guarded Heat Flow Meter Technique [6], using an Anter Quickline-10$^{TM}$ machine. The machine consists of a heater, an upper metal plate (surface of 50.8 mm diameter), a lower metal plate (surface of 50.8 mm diameter), a calorimeter

and a heat sink, shown in Figure 1. The sample to be measured that should have a 50.8 mm diameter flat surface is placed between the lower and upper plate and three thermistors read the temperatures of the upper plate, lower plate and heat sink.

The effective thermal conductivity of the sample is calculated using the following equation:

$$k = \frac{t}{R_{th}} \tag{1}$$

where $k$ is the effective thermal conductivity (W/(mK)), $t$ is the sample thickness (m) and $R_{th}$ is the sample thermal resistance ($m^2K/W$) that can be obtained from:

$$R_{th} = \frac{(T_u - T_l)}{Q} - R_{th,int} = \frac{F \cdot (T_u - T_l)}{(T_l - T_h)} - R_{th,int} = F \cdot \left(\frac{\Delta T_s}{\Delta T_r}\right) - R_{th,int} \tag{2}$$

where $T_u$ and $T_l$ a are the surface temperatures of the upper and lower plate respectively (K), $T_h$ is the heat sink temperature (K), $Q$ is the thermal flux through the test sample ($W/m^2$), $R_{th,int}$ is the total interfacial thermal resistance between the sample and the surface plates ($m^2K/W$), $F$ is the reference thermal resistance ($m^2K/W$), $\Delta T_s$ is the temperature difference across the sample (K) and $\Delta T_r$ is the temperature difference across the referenced calorimeter (K).

Before measuring the thermal conductivity of the samples, the Anter Quickline-10™ machine must be calibrated in their range of thermal resistance, so that the values $R_{th,int}$ and $F$ of Equation (2) can be obtained. The Anter Quickline-10™ machine is provided with a set of sample disks of known thicknesses and thermal conductivities used to calibrate the machine. A calibration line was done with the provided Vespel™ samples (two disks of diameter 50.8 mm and 3.175 mm and 6.35 mm thickness respectively). The thermal resistance range of this

calibration line was insufficient for the carbon samples and most of them would fall outside the range so a new calibration line with another low thermal conductivity material was done.

Because the carbon samples that were going to be measured had a square cross section, four square blocks of PEEK of 50.8 mm side and different thicknesses, 2.5 mm, 5 mm, 10 mm and 20 mm respectively were manufactured. The thinner block was measured (in between with two blocks of a high thermal conductivity metal that transform the upper and lower round surface plates of the machine into square ones) and according to the previous Vespel™ calibration it had a conductivity of 0.29 W/(mK). Knowing the thermal conductivity and the thicknesses of the PEEK blocks the calibration line was obtained and it is shown in Figure 2. The values of $F$ and $R_{th,int}$ were calculated as 0.0026 K/W and 0.0001 K/W respectively.

During the process of calibration and measuring samples the Anter Quickline-10™ machine has to be set and operate at the same boundary temperatures. In this case the machine is set to a high temperature of 55°C and a low temperature of 10°C.

The carbon samples thermal conductivities were measured using a square cross-section sample holder shown in Figure 3 that consists of two blocks of 50.8 mm x 50.8 mm x 10 mm made of a high thermal conductivity metal and four walls made of a low thermal conductivity polymer all linked with 24 bolts. With one of the walls removed, the carbon was placed inside the holder, creating a 5 mm block thickness sample, and could be compressed by hand using a suitable plunger. In this way the density of the sample could be better controlled. Once the compression process is finished the wall is placed back in the holder and the complete assembly is placed between the upper and lower plate of the Anter Quickline-10™ machine. The

experiment could take up to 3 h to run, depending on the sample thermal conductivity and thickness.

The two high thermal conductivity metal blocks were made of aluminium which has a conductivity of 237 W/(mK), three orders of magnitude higher than the carbon samples. The high conductivity of these blocks helps to transform the upper and lower surface plate of 50.8 mm diameter into square cross-section surfaces of 50.8 mm side necessary in order to measure square carbon samples.

To obtain the thermal conductivity of the carbon mixtures, measurements of the $T_u$, $T_l$ and $T_h$ shown in the Anter Quickline-10$^{TM}$ machine display were taken for each sample. For the experiment results to be accurate, every thermal resistance obtained must fall within the corresponding calibration range which goes from 0.012 to 0.069 m$^2$K/W (Figure 2). To avoid thermal contact resistances between the aluminium blocks and the upper and lower plates of the machine a high conductivity grease was applied to the surfaces and used in all the experiments.

In order to have more confidence with the tests done with the square flat plate holder, the assembly of aluminium blocks and carbon was drawn in SolidWorks$^{TM}$ and the steady state heat transfer software package within SolidWorks$^{TM}$ was used to simulate each result. The boundary conditions used in each simulation were the upper and lower temperature obtained from the Quickline-10$^{TM}$ machine applied in a circle of 50.8 mm diameter at each side of the sample holder, the rest of the surfaces that during the experiment were in contact with air were treated as adiabatic and the contact between the carbon and the aluminium was treated as a bond. The simulations show that there is a very low discrepancy, up to 3% in the effective thermal conductivity value.

**Steady State Experiments Accuracy**

The thermal conductivity of the samples is measured with the Anter Quickline-10$^{TM}$ machine with a global error that can vary between ±3% and ±8%, depending on the thermal resistance of the sample. The accuracy improves when the ratio between $R_{th,int}$ and $R_s$ is small.

In order to obtain the accuracy of the thermal resistance readings it must be taken into account that the Anter Quickline-10$^{TM}$ machine software converts the voltage measured by the three thermistors in the upper plate, lower plate and heat sink to temperature at a constant 7.045°C/V rate. The resolution of the voltage meter is 1 mV so the temperature resolution is 0.007°C. Calculating the reading error with typical values of the carbon samples it is possible to obtain a thermal resistance reading error of 0.179%.

**Transient Hot Tube Measurement**

The transient hot wire (or in this case, hot tube) technique is a well developed and widely used technique for measurements of thermal conductivity of fluids and solids [7, 8]. It consists of a tube of a resistive element immersed in the liquid or solid sample and the experiment is simply performed by recording the voltage change over the source/sensor element while its temperature is raised by an electrical current. The source element in this case is a stainless steel tube extracted from one of the sorption generators used for heat pumping purposes.

The temperature of the hot tube will depend on the electrical properties of the conducting material used and vice versa. The governing equation of the tube resistance, *R*, is:

$$R_{el}(t) = R_{el,0}\left(1 + \alpha \Delta T(time)\right) \quad (3)$$

where $\alpha$ is the temperature coefficient that relates the increase in resistance with the increase in temperature of the material (Ω/K), $\Delta T$ is the temperature difference of the tube between the initial temperature $T_0$ and a temperature at given time $t$ (K) and $R_0$ (Ω) is the resistance of the tube at the initial temperature that depends on the geometry of the hot tube and can be calculated from the following equation:

$$R_{el,0} = \rho_0 \frac{l}{A} \tag{4}$$

where $\rho_0$ is the electrical resistivity of the stainless steel tube at the initial temperature (Ωm), $l$ is the length of the hot tube (m) and $A$ is the cross section area of the hot tube ($m^2$).

When using the hot tube technique it is important to be aware of the influence from the outside of the sample boundaries. According to the hot tube theory it is assumed that the testing sample is infinitely large, is at an initial constant temperature and has no influence from the outside sample surfaces. The hot tube is located in the x axis inside this infinite solid that has an intrinsic thermal conductivity $\lambda$ (W/(mK)), a density $d$ (kg/$m^3$), a specific heat $C_p$ (J/(kgK)) and a heat transfer coefficient between the tube and the solid $h$ (W/($m^2$K)). With all this data and a simulation program is possible to obtain the temperature increase at any point $y$, $z$ around the tube and at any time.

The apparatus used to record the changes of resistance of the hot tube was the SourceMeter™ Line 2430, it is a source measurement unit instrument that provides precision voltage and current sourcing. Its working 4 wire principle is explained in Figure 4, in which $I$ is the applied current from the SourceMeter™ through the hot tube (A), $R_{el}$ is the electrical resistance of the hot tube (Ω), $R_{el,LEAD}$ are the electrical resistances of the connecting wires (Ω), $V_M$ is the voltage measured by SourceMeter™ (V) and $V_S$ is the voltage across the hot tube (V).

The main advantage of the 4 wire technique is that it minimizes the effects of Lead Resistances by measuring the voltage across the resistance under test ($V_R$) with a second set of test leads. Since the sense current used is very low (in the order of pA) the Lead Resistances of the second set are negligible and the measured voltage ($V_M$) is essentially the same as the voltage across the resistance under test.

$$R_{el} = \frac{V_R}{I} \approx \frac{V_M}{I} \quad (5)$$

To run this experiment with active carbon the heating wire and temperature sensor had to be encapsulated or insulated from the testing material as the active carbon is an electrical conductor. In this case the RS 199-1480 varnish was applied by dipping on the surface of the tube.

The transient hot tube measurement was carried out using two different sample holders:

- The first one comprises a plastic measurement cylinder (40 mm diameter and 300 mm height) with a 100 mm hot tube place in its axis. This sample holder was used to measure thermal conductivities and thermal resistances of vibrated carbon samples.
- The second one comprises a metallic box (75 mm depth, 150 mm height and 300 mm length) with a 240 mm hot tube placed in longitudinally. This sample holder was used to measure thermal conductivities and thermal resistances of mechanically compressed carbon samples.

For the chosen experiment time (60 s) the heated wave in the carbon never breaks through the boundaries of the samples, otherwise a shorter experiment time should be chosen.

In all the experiments the applied current in the tube was 3 A and the environmental conditions were 20 °C and atmospheric pressure.



 

**Accuracy of the experiments**

The SourceMeter™ unit has detailed information in its manuals about the accuracy of the reading for different currents sources and voltage measurements. The applied current for all the experiments was 3 A with a source resolution of 500 nA, the measured voltages vary from 0.37 to 0.89 V with a measurement resolution of 10 μV and the sampling time was 0.2 s. The current source accuracy is: $\pm(0.045\% * I + 2\mu)\ A$; the voltage measurement accuracy is: $\pm(0.067\% * V + 300\mu)\ V$. Operating with the known experimental values it is possible to obtain the accuracy of the measured resistances. In the case of the short hot tube (100 mm) the accuracy is: $\pm 0.150\% * R\ \Omega$. For the long hot tube (240 mm) the accuracy is: $\pm 0.106\% * R\ \Omega$.

**Active Carbon Specifications**

The granular carbon and the carbon powder used in the experiments were supplied by Chemviron Carbon Ltd., both being type 208C based on coconut shell precursor.

Carbon specifications:

- **20 x 40 USS** (Carbon grains can pass through a sieve opening of 850 μm but not through an opening of 425 μm): Maximum granular bulk density after a vibrating process of 527 kg/m$^3$.
- **Greater than 80 USS** (Powder, carbon grains that can pass through a sieve opening of 180 μm): Maximum granular bulk density after a vibrating process of 544 kg/m$^3$.

The thermal conductivity and thermal resistance of the previous two carbon grades were measured on their own and then three binary mixtures of 66.7% grains - 33.3% powder,

50.0% grains - 50.0% powder and lastly 33.3% grains - 66.7% powder (by weight) were measured.

Before conducting a test the carbon must be dried to eliminate the moisture that could be adsorbed from the surrounding air. It is sufficient to leave the carbon for 30 min at 150 °C in a furnace.

***TRANSIENT HOT TUBE MATHEMATICAL MODELLING***

A computational simulation was written in Matlab™ in order to analyse the resistance results obtained in the transient hot tube experiments. It consists of a one dimensional finite difference model in which the stainless steel tube and the varnish layer are represented by single elements and the active carbon in which the tube is immersed is represented as a grid of concentric layers to the tube axis. The model can be schematically represented in Figure 5.

where $h$ is the heat transfer coefficient of the air layer that surrounds the hot tube (W/(m$^2$K)) and $\lambda$ is the intrinsic thermal conductivity of the surrounding carbon (W/(mK)).

When modelling the experiment in this way, with a heat transfer coefficient and an intrinsic thermal conductivity, the simulation produces more accurate results and makes possible to investigate the effect of the wall contact resistance between the different samples and the tube.

The air heat transfer coefficient is defined by the Equation (6).

$$h = \frac{k_{air}}{t} \tag{6}$$

where $k_{air}$ is the air thermal conductivity (W/(mK)) and $t$ is the air layer thickness that surrounds the hot tube (m).



 

The stainless steel tube used in the experiments has an outer diameter of 1.2 mm and an inner diameter of 0.8 mm, and the thickness of the varnish layer is 0.05 mm.

The following table, Table 1 [9-11], shows the thermo physical properties of the stainless steel and varnish needed to simulate the experiments.

Before starting the hot tube experiments the $R_{el,0}$ of the tube should be measured. In order to do that, a low electrical current, 10 mA, was applied to the tube and the resistance value was measured to be 1.1982 Ω/m. The resistance temperature coefficient of the stainless steel, α, found from the literature is 0.00112 Ω/K [9].

As the thermal conductivity of the air depends on the temperature and ambient pressure, the value used in the simulations is 0.0321 W/(mK) that corresponds to a temperature of 40 °C (313 K), an average of the tube temperature during the experiments and to atmospheric pressure [12].

The specific heat capacity of the carbon at constant pressure (J/(kgK)) is found to be a function of its temperature in Kelvin and it is defined in Equation (7) [13].

$$C_p = 175 + 2.245 \cdot T(time) \quad (7)$$

***RESULTS AND DISCUSSION***

As in the steady state flat plates experiments only the effective thermal conductivity of the samples was obtained, to be able to compare it with the intrinsic thermal conductivity measured from the transient hot tube experiments, they should be transformed into intrinsic thermal conductivities. This could be done by applying the correspondent heat transfer coefficient of the hot tube tests (for each type of mixture and density) to the Anter Quickline-10$^{TM}$ results using the Equation (8).

$$\lambda = \frac{t}{\frac{t}{k} - \frac{2}{h}} \quad (8)$$

where *t* is its carbon sample thickness (m), *k* is the effective thermal conductivity (W/(mK)) and *h* is the heat transfer coefficient of the air layer (W/(m$^2$K)) that surrounds the hot tube that in this case would correspond to a wall contact resistance of the upper and lower surfaces of the square carbon sample.

Once the intrinsic thermal conductivities of both flat plates and hot tube experiments are known they could be compared in Figure 6. The intrinsic thermal conductivities of different mixtures, grains and powder, from both experiments are plotted against their density and it can be seen that both follow the same trend, higher thermal conductivities at higher densities, and that both techniques produce practically the same results.

In Figure 7 the intrinsic thermal conductivities obtained from the transient hot tube experiments are plotted for the different grains and powder mixtures, 100% grains, 66.7% grains – 33.3% powder, 50% grins – 50% powder, 33.3% grains – 66.7% powder and 100% powder. The highest thermal conductivities correspond to the binary mixtures of grains and powder that as well show the highest densities. The 20x40 grains and powder samples on their own show a poor thermal conductivity performance.

In Figure 8 the contact air layer thickness of every sample mixture is plotted against its density. The trend that can be observed is that for each sample the higher the density the thinner the air contact layer.

***COMPARISON WITH THEORETICAL MODELS***

In order to have more confidence with the results obtained in the tests, these were compared with different theoretical models of thermal conductivity for porous beds.

The first model studied is the geometric mean model that assumes a random distribution of phases. The thermal conductivity of the bed is given by the weighted geometric mean of the conductivities of the carbon grains and the air:

$$k_{bed} = {k_{grain}}^{1-\varepsilon}\, {k_{air}}^{\varepsilon} \tag{9}$$

where $k_{grain}$ is the thermal conductivity of a piece of active carbon (0.85 W/(mK)), $k_{air}$ is the thermal conductivity of the air (0.0321 W/(mK)) and $\boldsymbol{\varepsilon}$ is the porosity of the bed (depends on the sample density).

The second model is the Krupiczka model [14] that consists of an approximated general correlation based on the porosity of the bed, $\boldsymbol{\varepsilon}$.

$$k_{bed} = k_{air}\left(\frac{k_{grain}}{k_{air}}\right)^{a+b\log\left(\frac{k_{grain}}{k_{air}}\right)} \tag{10}$$

where

$$a = 0.28 - 0.7571\, log\varepsilon \qquad \text{and} \qquad b = -0.057.$$

The third model corresponds to the Woodside and Messmer model [15]. It combines both series and parallel heat transfer distribution (layers of carbon and air perpendicular or parallel to the heat flux) and electrical conductivity analogy.

$$k_{bed} = \frac{b\, k_{grain}\, k_{air}}{k_{grain}(1-c)+c\, k_{air}} + a\, k_{grain} \tag{11}$$

where

$$a = \varepsilon - 0.03, \qquad b = 1 - a \qquad \text{and} \qquad c = \frac{1-\varepsilon}{a}.$$

The fourth and last model studied corresponds to the Zehner and Schlunder model [16] which assumes point contacts between spherical particles in one dimension heat flow.

$$k_{bed} = k_{air}\left(1-(1-\varepsilon)^{0.5}+\frac{2(1-\varepsilon)^{0.5}}{1-ab}\left(\frac{(1-a)b}{(1-a\,b)^2}\,ln\left({}^{1}/_{a\,b}\right)-\frac{b+1}{2}-\frac{b-1}{1-a\,b}\right)\right) \qquad (12)$$

where

$$a=\frac{k_{grain}}{k_{air}} \qquad \text{and} \qquad b=1.25\left(\frac{1-\varepsilon}{\varepsilon}\right)^{\frac{10}{9}}$$

The theoretical values obtained were plotted along with the flat plates and hot tube test results for the non-binary samples, the 100% 20x40 grains and the 100% powder. Only non-binary samples were compared because they present a more homogenous size distribution than the mixtures of grains and powder.

From Figure 9 can be observed that the Krupiczka model is the one that fits better with the 100% 20x40 grains sample. In Figure 10 the models that fit better the 100% powder sample are the Geometric mean and the Zehner and Schlunder [16] one. The other models compared predict thermal conductivities higher of lower that the tests.

The differences between experimental and theoretical values could be due to the fact that the carbon particles shapes are very irregular in contrast to the spherical particles of the models. As well, regarding the size distribution of the samples, even though they are not a grain-powder mixture, they do present a size variation (see Active Carbon Specifications section).

***CONCLUSIONS***

The intrinsic thermal conductivities of the steady state flat plates experiments were very similar to the ones corresponding with the transient hot tube experiments if to the first ones were applied the same heat transfer coefficients (or wall contact resistance) of the second ones. This indicates that on one side, both experiments are comparable and achieve the same results and on the other side that the wall contact resistance of the flat plates and the 1.2 mm diameter tube is practically the same.

The binary mixtures of grains and powder can achieve higher densities, up to 745 $kg/m^3$, and as a consequence higher thermal conductivities, 0.33 W/(mK), at the same vibration or compression rates than grains or powder on their own. In the case of the 100% grain samples, the thermal conductivity variation with density is almost negligible as it only varies from 0.23 W/(mK) to 0.24 W/(mK) from loose, 444 $kg/m^3$, to mechanically compressed samples, 526 $kg/m^3$. The powder is the sample that shows the lowest thermal conductivity, it varies with density but only from 0.12 W/(mK) at 375 $kg/m^3$ to 0.17 W/(mK) at 556 $kg/m^3$. This could be due to the high number of point contacts in the sample (a high percentage of the particle sizes are comprised between 5 and 50 μm); further research will be done to clarify this.

The contact air layer thickness between the samples and the hot tube or wall contact resistance decreases with the density of the sample. The 100% grain samples show a sharp drop in wall contact resistance with density while the 100% powder samples seem to progressively stabilise in a wall contact resistance. The grains and powder mixture samples seem to follow this trend, the higher the percentage of grains in the mixture the sharper the drop in wall contact resistance.

The mechanically compressed samples in the results correspond to the two highest densities samples in the 66.7% grains and 33.3% powder and the highest density sample in the 100% grains sample. The compressed results follow the general trend of increase in thermal conductivity in relation with density at the same rates of vibrated samples. Regarding the contact air layer thickness, in the case of the grains the air layer drops sharply with mechanical compression whilst in the compressed mixture samples the air layer tends to smoothly stabilise for higher densities.

More experiments with higher densities will be conducted to obtain a complete map of wall contact resistances and achieve a better understanding of the interaction of the bulk thermal conductivity with the geometry of the wall.

***ACKNOWLEDGEMENT***

Science City Research Alliance for the use of the Quickline-10 ™ machine and the SourceMeter™ and Chemviron Carbon LTD for supplying the active carbon used in the experiments.



 

***NOMENCLATURE***

| | |
|---|---|
| $A$ | Cross section area, $m^2$ |
| $C_p$ | Specific heat at constant pressure, J/(kgK) |
| $d$ | Density, $kg/m^3$ |
| $F$ | Reference thermal resistance, $m^2K/W$ |
| $h$ | Heat transfer coefficient, $W/(m^2K)$ |
| $I$ | Electrical current, A |
| $k$ | Effective thermal conductivity, W/(mK) |
| $l$ | Length, m |
| $Q$ | Thermal flux, $W/m^2$ |
| $R_{el}$ | Electrical resistance, Ω |
| $R_{th}$ | Thermal resistance, $m^2K/W$ |
| $T$ | Temperature, K |
| $t$ | Thickness, m |
| $V$ | Voltage, V |



 

***Greek Symbols***

| | |
|---|---|
| $\alpha$ | Temperature coefficient, Ω/K |
| $\boldsymbol{\varepsilon}$ | Porosity, dimensionless |
| $\lambda$ | Intrinsic thermal conductivity, W/(mK) |
| $\rho$ | Electrical resistivity, Ωm |

***Subscripts***

| | |
|---|---|
| *0* | Initial |
| *h* | Heat sink |
| *int* | Interfacial |
| *l* | Lower plate |
| *LEAD* | Lead resistances |
| *M* | Electrical lead resistance and resistance under test |
| *r* | Referenced calorimeter |
| *R* | Electrical resistance under test |
| *s* | Sample |
| *u* | Upper plate |



 

***REFERENCES***

[1] Wang, L. W., Wang, R. Z., Lu, Z. S., Chen, C. J., Wang, K. and Wu, J. Y., The performance of two adsorption ice making test units using activated carbon and a carbon composite as adsorbents, *Carbon*, Vol. 44, pp. 2671-2680, 2006.

[2] Critoph, R. E., Turner, L., Heat transfer in granular activated carbon beds in the presence of adsorbable gases, *Int. J. Heat Mass Transfer*, Vol. 38, pp. 1577-1585, 1995.

[3] Waszkiewicz, S., Jenkins, S., Saidani-Scott, H., Tierney, M., Analysis of a finned heat exchanger working in an adsorption refrigeration system using zeolite and methanol, *Heat Transfer Engineering*, Vol. 24, No. 6, pp 71-78, 2003.

[4] Critoph, R. E., Metcalf, S. J., Tamainot-Telto, Z., Proof of concept car adsorption air-conditioning system using a compact sorption reactor, *Heat Transfer Engineering*, Vol. 31, No. 11, pp 950-956, 2010.

[5] Han, X. H., Wang, Q., Park, Y. G., T'joen, C., Sommers, A., Jacobi, A., A review of metal foam and metal matrix composites for heat exchangers and heat sinks, *Heat Transfer Engineering*, Vol. 33, no 12, pp 991-1009, 2012.

[6] ASTM E1530 Standard, Standard Test Method for Evaluating the Resistance to Thermal Transmission of Materials by the Guarded Heat Flow Meter Technique, ASTM International, West Conshohocken, PA, 2011.

[7] Healy, J. J., de Groot, J. J., Kestin, J., The theory of the transient hot-wire method for measuring thermal conductivity, *Physica B+C*, Vol. 82, No. 2, pp 392-408, 1976.



 

[8] Franco, A., An apparatus for the routine measurement of thermal conductivity of materials for building application based on a transient hot-wire method, *Applied Thermal Engineering*, Vol. 27, pp 2495-2504, 2007.

[9] Graves, R. S., Kollie, T. G., McElroy, D. L., and Gilchrist, K. E., The thermal conductivity of AISI 304L Stainless Steel, *International Journal of Thermophysics*, Vol. 12, No. 2, 1991.

[10] Safety data sheet insulating varnish, CP0247 v2.3 RS 199-1480, Report date: 13/05/2010.

[11] Totten, G. E., Westbrook, S. R., Shah R. J., Fuels and lubricants handbook: technology, properties performance and testing, ASTM International, 2003.

[12] Lemmon, E. W. and Jacobsen, R. T., Viscosity and thermal conductivity equations for nitrogen, oxygen, argon and air, *International Journal of Thermophysics*, Vol. 25, No. 1, 2004.

[13] Tamainot-Telto, Z. and Critoph, R. E., Monolithic carbon for sorption refrigeration and heat pump applications, *Applied Thermal Engineering*, Vol. 21, pp. 37-52, 2001.

[14] Krupiczka, R., Analysis of thermal conductivity in granular materials, *Int. Chem. Eng.*, Vol. 7, pp 122-144, 1967.

[15] Woodside, W., Messmer, J. H., Thermal conductivity of porous media. I. Unconsolidated sands, *Journal of Applied Physics*, Vol. 32, pp 1688, 1961.

[16] Zehner, P., Schlunder, E. U., Thermal conductivity of granular materials at moderate temperatures, *Chemie Ingenieur Technik*, Vol. 42, pp 933-941, 1970.



 

Table 1 Thermophysical properties of the materials used in the modelling [9-11]

| | **Stainless steel** | **Varnish** |
|---|---|---|
| **Density (kg/m$^3$)** | 7873 | 920 |
| **Specific heat (J/(kgK))** | 485 | 2090 |
| **Thermal conductivity (W/(mK))** | 16.2 | 0.12 |



 

***List of figure captions***





 

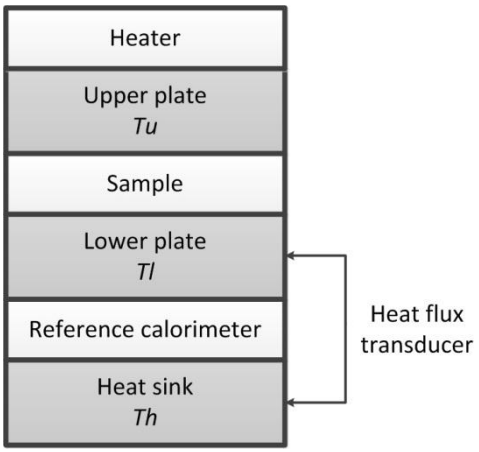


Figure 1 Thermal conductivity principle of the Anter Quickline-10$^{TM}$ machine



 

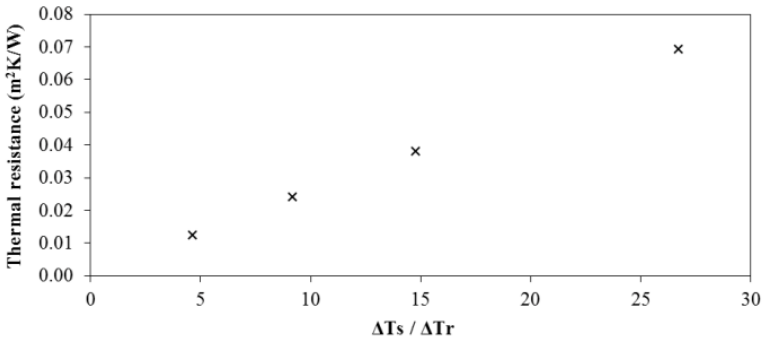


Figure 2 Square PEEK samples calibration line



 

Figure 3 Steady state flat plates sample holder



 

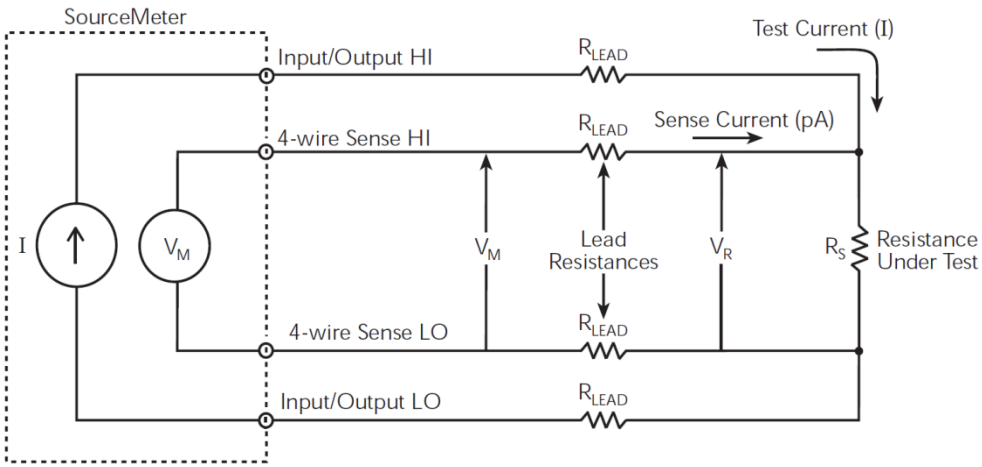


Figure 4 4-Wire SourceMeter™ resistance sensing diagram

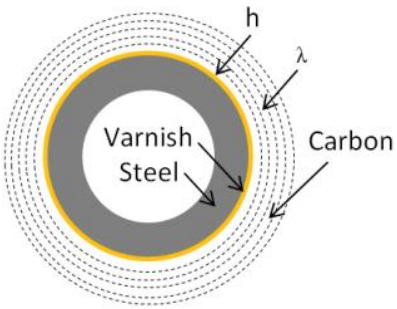


Figure 5 Cross section drawing of the hot tube test

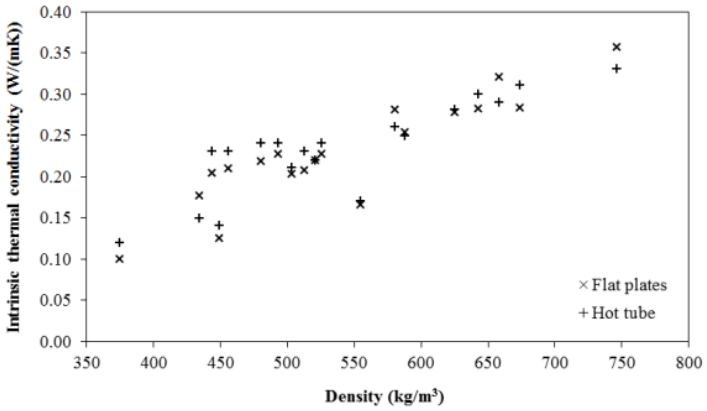


Figure 6 Thermal conductivity results comparison of steady state flat plates and dynamic hot tube for different 20x40 grains and powder mixtures

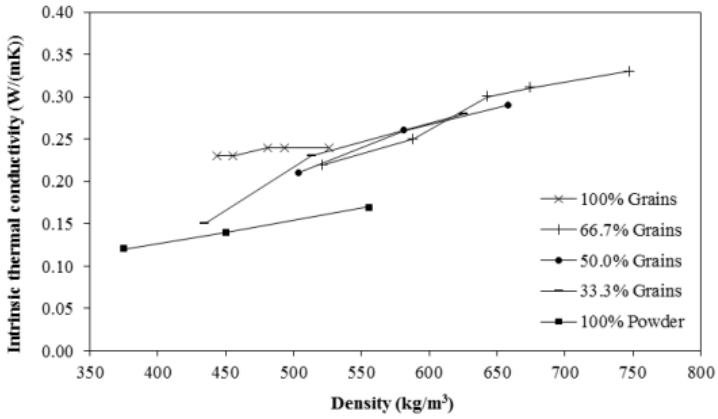


Figure 7 Thermal conductivity of different 20x40 grains and powder mixtures

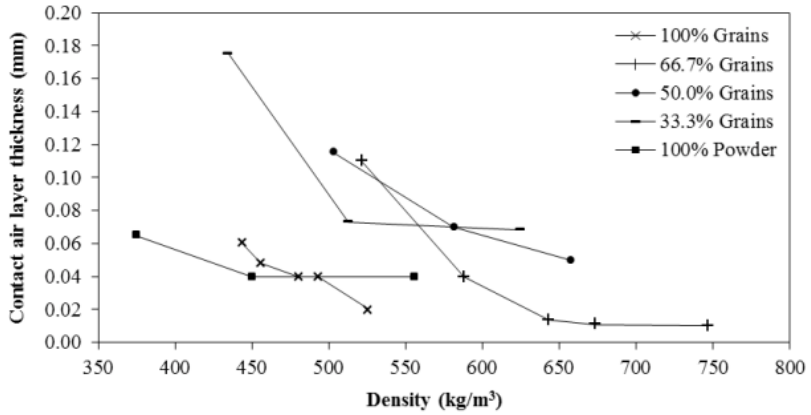


Figure 8 Contact air layer thickness between hot tube and different 20x40 grains and powder mixtures



 

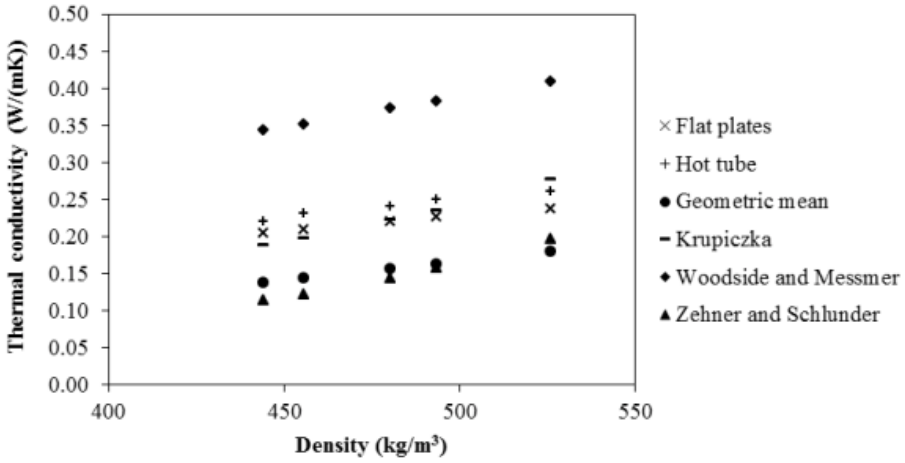


Figure 9 Thermal conductivity comparisons of experiments and theoretical models {Geometric mean, Eq. (9), Krupiczka [14], Woodside and Messmer [15] and Zehner and Schlunder [16]}, for 100% 20x40 grains sample



 

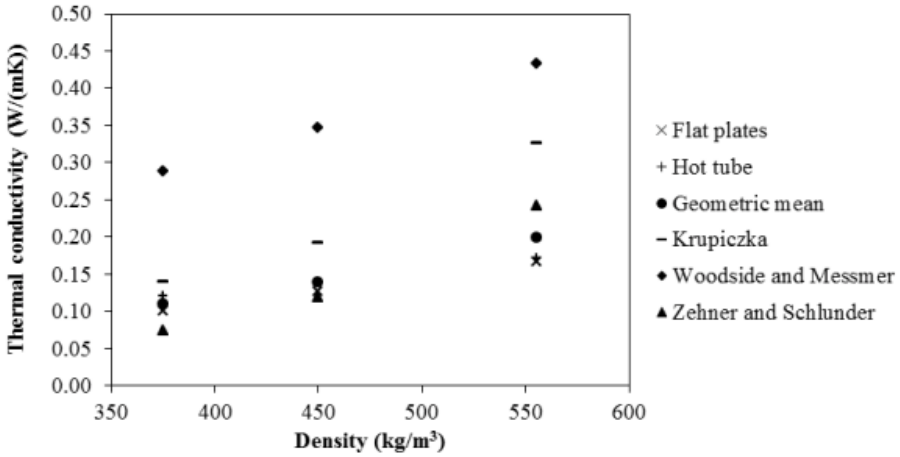


Figure 10 Thermal conductivity comparison of experiments and theoretical models {Geometric mean, Eq. (9), Krupiczka [14], Woodside and Messmer [15] and Zehner and Schlunder [16]}, for 100% powder

**Angeles Rivero Pacho** is a research engineer at the SEED, Sustainable Energy Engineering and Design, group at the University of Warwick, Coventry, United Kingdom, under the supervision of Prof. Robert Critoph. She received her Ph.D. degree from the University of Warwick, UK, her M.Sc. degree from Cranfield University, UK, and her M.Eng. degree from the Polytechnic University of Valencia, Spain. She is currently working on the development of a solid sorption heat pump.

**Robert Critoph** is a Professor of Thermal Sciences at the University of Warwick, Coventry, United Kingdom. He is the Head of Sustainable Energy Engineering and Design and the Energy Theme Leader. He received his B.Sc. and Ph.D. degrees from the University of Southampton, Southampton, UK. He has worked on heat pump and refrigeration systems since 1982, published about 90 papers, 2 book chapters, 5 patents and managed contracts worth £5M for industry, government and the EU. Industrial clients have included British Gas, Searle and Unilever. He is currently directing i-STUTE, an interdisciplinary centre for storage, upgrading and transformation of thermal energy.

**Steven Metcalf** is a research engineer at the SEED, Sustainable Energy Engineering and Design, group at the University of Warwick, Coventry, United Kingdom. He received his M.Eng. and Ph.D. from the University of Warwick. He is currently developing a gas fired adsorption heat pump designed to replace a domestic gas boiler.